

5-17-2013

Visible-light photoresponse of AlN-based film bulk acoustic wave resonator

Changjian Zhou

Yi Yang

Y. Shu

Hualin Cai

Tian-Ling Ren

See next page for additional authors

Follow this and additional works at: <https://scholarcommons.scu.edu/elec>

Recommended Citation

C.J. Zhou, Y. Yang, Y. Shu, H.L. Cai, T.L. Ren, M. Chan, J. Zhou, H. Jin, S.R. Dong, and C.Y. Yang, "Visible-light photoresponse of AlN-based film bulk acoustic wave resonator," *Applied Physics Letters* 102, 191914 (3 pp) (2013). <https://doi.org/10.1063/1.4807135>

Copyright © 2013 American Institute of Physics Publishing. Reprinted with permission.

This Article is brought to you for free and open access by the School of Engineering at Scholar Commons. It has been accepted for inclusion in Electrical Engineering by an authorized administrator of Scholar Commons. For more information, please contact rscroggin@scu.edu.

Authors

Changjian Zhou, Yi Yang, Y. Shu, Hualin Cai, Tian-Ling Ren, Mansun Chan, J. Zhou, Hao Jin, Shurong Dong, and Cary Y. Yang

Visible-light photoresponse of AlN-based film bulk acoustic wave resonator

C. J. Zhou,^{1,2} Y. Yang,¹ Y. Shu,¹ H. L. Cai,¹ T. L. Ren,^{1,a)} M. Chan,² J. Zhou,³ H. Jin,³ S. R. Dong,³ and C. Y. Yang⁴

¹*Institute of Microelectronics, Tsinghua University, Beijing 100084, China*

²*Department of Electronic and Computer Engineering, Hong Kong University of Science and Technology, Clear Water Bay, Hong Kong*

³*Department of Information Science and Electronic Engineering, Zhejiang University, Hangzhou 310027, China*

⁴*Center for Nanostructures, Santa Clara University, Santa Clara, California 95053, USA*

(Received 13 April 2013; accepted 3 May 2013; published online 17 May 2013)

Visible-light photoresponse of an AlN-based film bulk acoustic wave resonator (FBAR) is demonstrated. It is found that the FBAR exhibits a resonant frequency downshift under purple light illumination and the magnitude of the frequency downshift increases as the power density increases within the range of 5–40 mW/cm². A resonant frequency downshift of 1313 KHz is observed under 40 mW/cm² illumination, corresponding to a minimum detection power of 6.09 nW. A sub-bandgap photoresponse of the AlN thin film is proposed to explain this phenomenon. © 2013 AIP Publishing LLC. [<http://dx.doi.org/10.1063/1.4807135>]

Film bulk acoustic wave resonators (FBARs) have been widely used for wireless communications as filters and duplexers,¹ and numerous sensing applications such as pressure sensors,² gas sensors,³ biosensors,⁴ and photoelectric sensors.⁵ Due to their high operating frequency and digital output characteristics, FBAR-based microsensors are very promising for constructing the sensor nodes for wireless applications. Recently, the development of optical communication requires high-speed, compact photoelectric sensors for optical front-end module.⁶ Commonly used piezoelectric thin films in acoustic wave devices such as ZnO and AlN are wide-bandgap semiconductors. Their sensitivities to illumination result in the resonant frequency shift for the acoustic wave devices. Several authors have reported the effect of ultraviolet radiation on ZnO-based FBARs and ZnO, GaN, and AlGaN-based surface acoustic wave devices.^{5,7–10} It is noteworthy that different combinations of materials and light source wavelengths were used in those studies, suggesting that indirect-bandgap photoresponses are responsible for the resonant frequency shift observed. Those experimental results indicate that it might be possible to develop visible-light photosensors based on the fabricated devices. In view of the potential applications of FBARs to visible-light communications, integration of visible-light sensor with wireless filter can provide a cost-effective solution to implement an optical front-end module.

Unlike ZnO, AlN is CMOS-compatible and chemically stable, which is the primary motivation for using it for this study. The working frequency of the AlN-based FBARs is chosen to be around 2.4 GHz, a standard ISM band for wireless communications. In this letter, the design and fabrication of the test device are described and the mechanisms underlying the frequency shifts for different photon wavelengths are discussed.

The test device is fabricated using a 4 in. silicon wafer with a 400 nm thermally oxidized SiO₂ as the starting

substrate. The bottom electrode Pt/Ti (150 nm/30 nm) and the top electrode Au/Cr (50 nm/10 nm) are deposited using e-beam evaporation and patterned with a lift-off process. The piezoelectric AlN film with a thickness of ~1 μm is deposited with DC reactive sputtering. The sputtering conditions, power, N₂/Ar gas flow rate, and substrate temperature are optimized to obtain a c-axis-oriented AlN film. Cavities are formed by etching off the SiO₂ film surrounding the resonant structure. By using the XeF₂ as the etching agent, the final resonant structure is obtained after etching off the silicon substrate beneath the supporting SiO₂ film.

Figure 1(a) shows the schematic cross-section of the AlN-based FBAR (not to scale), and Fig. 1(b) is the top-view photograph of a fabricated FBAR. The middle elliptical region is the resonant area (~0.01 mm²) with the AlN film sandwiched between the bottom and the top electrodes. The surface morphology and the orientation of the AlN film are characterized using atomic force microscopy (AFM) and X-Ray diffraction (XRD), respectively. The AFM image of the AlN film is shown in Fig. 1(c), with a RMS roughness of 5.7 nm. Figure 1(d) shows the XRD spectrum of the AlN film on the Pt/Ti bottom electrode. Only (002) crystalline orientation is observed for AlN, indicating the AlN film exhibits the preferred c-axis orientation which is critical for achieving high-performance FBARs.

First, the frequency response of the FBAR reflection coefficient S_{11} in the dark is measured using a vector network analyzer and microprobe station. The IFBW is at 100 Hz and 1601 data points are obtained over the specified frequency range. Figure 2(a) shows the S_{11} parameter for a typical FBAR. For this device, the serial resonant frequency (f_s) and parallel resonant frequency (f_p) are 2.395 GHz and 2.449 GHz, respectively, yielding a coupling coefficient K_{eff}^2 of 5.39%, where $K_{eff}^2 = \frac{\pi^2}{4} \left(\frac{f_p - f_s}{f_p} \right)^2$. The quality factor at the resonant peak (2.409431 GHz) is 485, calculated from the measured results using the phase gradient method.⁵

Next the photoresponse of the FBAR to visible light is characterized at wavelengths of 650 nm (red), 532 nm (green), and 405 nm (purple), respectively. The initial power

^{a)}Author to whom correspondence should be addressed. Electronic mail: RenTL@tsinghua.edu.cn

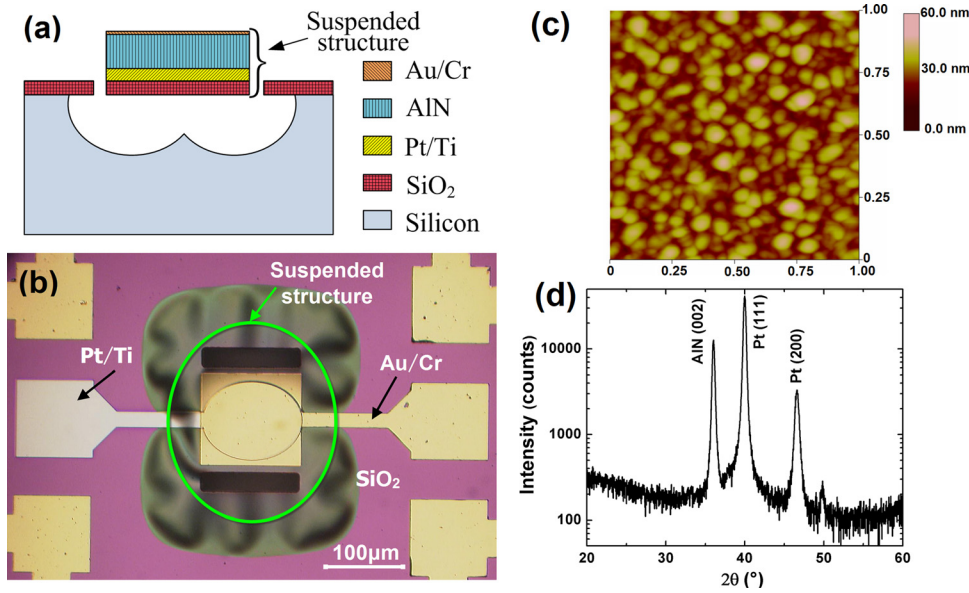


FIG. 1. (a) Schematic cross-section of AlN-based FBAR (not to scale). (b) Top-view photograph of a fabricated FBAR. (c) AFM image of AlN film surface morphology. (d) XRD spectrum of AlN film on Pt/Ti bottom electrode.

density of the laser is set at 5 mW/cm^2 . The spanned frequency range is 3 MHz with the center frequency at the resonant peak of S_{11} . This gives rise to a noise floor of $\sim 2 \text{ kHz}$ for the number of data points measured. The measured data are to reveal small resonant frequency shifts due to illumination, as shown in Fig. 2(b). When the FBAR is illuminated with green or red laser, there is no resonant frequency shift but only a small difference in the S_{11} magnitude. However, a

frequency downshift of 123 kHz appears when the sample is illuminated with purple light.

To study the dependence of the frequency shift on the power density of the purple light, we have characterized the FBAR with power densities between 5 mW/cm^2 and 40 mW/cm^2 , and the results are shown in Figure 3. The frequency downshift increases with increasing power density of the purple light, with a downshift of 1313 KHz at 40 mW/cm^2 . This corresponds to a minimum detection power of 6.09 nW , assuming a resonant area of 0.01 mm^2 . It is important to note that the S_{11} spectrum returns to its dark version immediately after the light is turned off, indicating a fast response of the AlN-based FBAR to illumination.

Before examining the exact origin of the visible-light photoresponse of the AlN-based FBAR, we have determined that the observed frequency downshift is not due to the temperature change of the FBAR. The time required for obtaining a S_{11} spectrum is less than 1 s and the frequency downshift occurs instantaneously after the light is turned on. Even if the entire laser energy is converted to heat, the temperature increase will not exceed 0.3°C when the laser power density

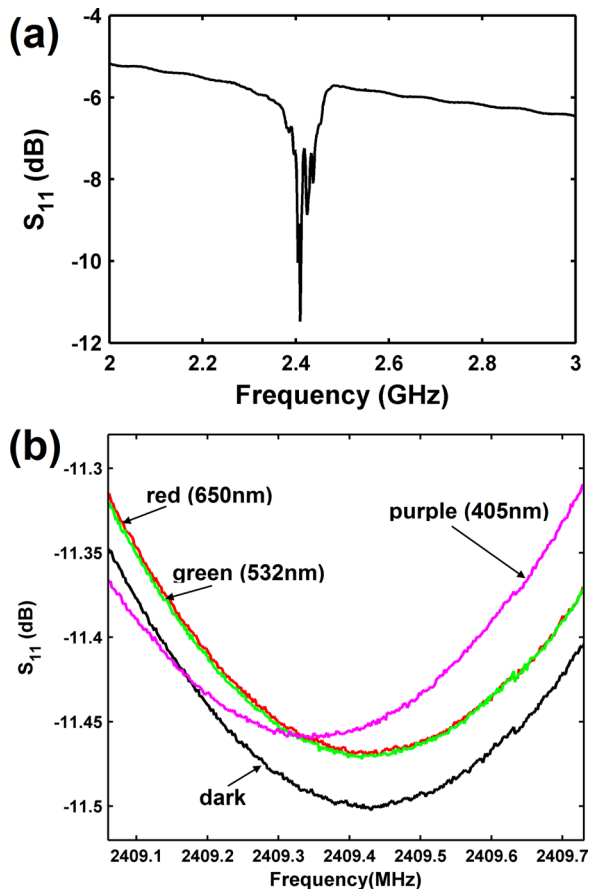


FIG. 2. (a) Measured S_{11} for an AlN-based FBAR in the dark; (b) S_{11} spectra for an AlN based FBAR under illumination at three wavelengths.

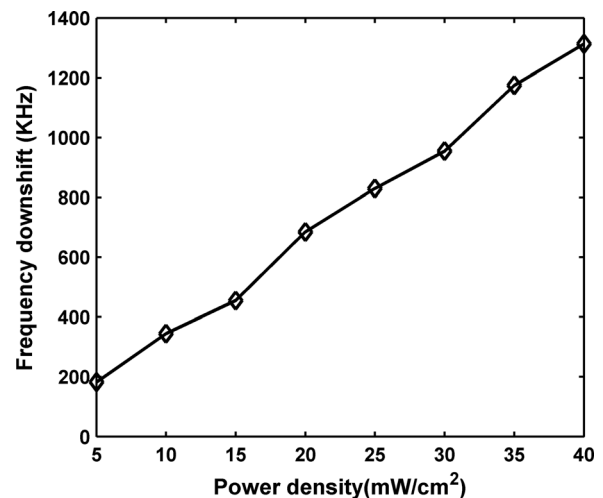


FIG. 3. Resonant frequency downshift of an AlN-based FBAR versus purple light power density.

is 40 mW/cm². Assuming a temperature coefficient of −19.5 ppm/°C for the fabricated AlN-based FBAR, this temperature increase will induce a frequency shift of at most ∼14 kHz, which is two orders of magnitude lower than the frequency downshift observed in the experiment.

Generally, the resonant frequency of the FBAR is given by $f_0 = v_a/2d$, where d is the AlN thickness and v_a its acoustic velocity given by $v_a = \sqrt{\frac{C_{33} + e^2/\epsilon_3}{\rho}}$, with C_{33} and ϵ_3 being the elastic and dielectric constants along the thickness direction, respectively, and e the piezoelectric constant. We argue as follows that the sub-bandgap photoresponse of the AlN thin film is the origin of the observed frequency downshift under purple illumination. AlN is a direct-gap semiconductor with a bandgap of 6.2 eV (corresponding to photon wavelength of 200 nm), and using doped single-crystal AlN thin film for 210 nm deep-ultraviolet laser emission has been reported.¹¹ In our study, the illumination laser is in the visible range, suggesting that the photoresponse of the FBAR is not due to the direct bandgap because of the much lower photon energies used. Since the AlN film used in this study is polycrystalline, it is very likely that photoresponses from states in the bandgap due to the defects such as oxygen and nitrogen vacancies in the sputtered film are responsible for the significant frequency downshift. Further, ultraviolet emission with wavelengths longer than 200 nm was obtained utilizing AlN nanostructures synthesized by different methods.^{12,13} When the AlN thin film is illuminated with purple light, the photo-generated charge carriers contribute to an increase in the capacitance of the AlN film. This is equivalent to an increase in the dielectric constants ϵ_3 , which in turn decreases the acoustic velocity propagated along the thickness direction. Accordingly, the resonant frequency of the AlN-based FBAR decreases.

To extract changes in the dielectric constants, the measured S-parameters are converted to admittance or Y-parameters. The imaginary part of the input admittance is mainly due to the static capacitance of the FBAR at a lower frequency than the resonant frequency. An estimation of the decrease in acoustic velocity due to the change of static capacitance is presented as follows.

Consider the case of 40 mW/cm² power density resulting in a downward frequency shift of 1313 kHz, the increase in the static capacitance is 1.3% (ωC_0 changes from 0.0153 S to 0.0155 S at 1 GHz). Using the material constants of AlN:¹⁴ $\rho = 3260 \text{ kg/m}^3$, $C_{33} = 395 \text{ GPa}$, $\epsilon_3 = 11$, and $e = 1.55$, the dark acoustic velocity and the acoustic velocity under illumination are computed as 11346 m/s and 11342 m/s, respectively, yielding a frequency downshift of 892 kHz. There is a

small discrepancy between the measured downshift of 1313 kHz and this estimated value, which is attributed to frequency dependence of the static capacitance. Since we cannot determine directly the static capacitance near the resonant frequency because of acoustoelectric interference, the static capacitance extracted at a lower frequency is probably slightly different from that closer to the resonant frequency. Nevertheless, such estimation confirms the validity of the proposed mechanism that provides a simple interpretation of the visible-light sensitivity of the AlN-based FBAR.

In summary, AlN-based FBAR with a working frequency of 2.4 GHz has been designed and fabricated and its photoresponse to various visible-light illuminations has been studied. While there is no observed frequency shift under red and green illumination, a resonant frequency downshift of 1313 kHz is observed under purple illumination with 40 mW/cm² power density, corresponding to a minimum detection power of 6.09 nW. A sub-bandgap photoresponse of the AlN thin film due to the presence of defects is proposed to explain this visible-light photoresponse phenomenon.

This work is supported by National Natural Science Foundation (61025021, 60936002, and 61020106006), and National Key Project of Science and Technology (2011ZX02403-002) of China.

¹R. Ruby, P. Bradley, J. Larson III, Y. Oshmyansky, and D. Figueredo, in *2001 IEEE International Solid-State Circuits Conference (IEDM)* (IEEE, 2001), p. 120.

²X. L. He, L. Garcia-Gancedo, P. C. Jin, J. Zhou, W. B. Wang, S. R. Dong, J. K. Luo, A. J. Flewitt, and W. I. Milne, *J. Micromech. Microeng.* **22**, 125005 (2012).

³R. Martins, E. Fortunato, P. Nunes, I. Ferreira, A. Marques, M. Bender, N. Katsarakis, V. Cimalla, and G. Kiriakidis, *J. Appl. Phys.* **96**, 1398 (2004).

⁴Z. Yan, X. Y. Zhou, G. K. H. Pang, T. Zhang, W. L. Liu, J. G. Cheng, Z. T. Song, S. L. Feng, L. H. Lai, J. Z. Chen, and Y. Wang, *Appl. Phys. Lett.* **90**, 143503 (2007).

⁵X. Qiu, J. Zhu, J. Oiler, C. Yu, Z. Wang, and H. Yu, *Appl. Phys. Lett.* **94**, 151917 (2009).

⁶S. Assefa, S. Shank, W. Green, M. Khater, E. Kiewra, C. Reinholm, S. Kamlapurkar, A. Rylyakov, C. Schow, F. Horst *et al.*, in *2012 IEEE International Electron Devices Meeting (IEDM)* (IEEE, 2012), p. 809.

⁷D. Ciplys, R. Rimeika, M. S. Shur, S. Rumyantsev, R. Gaska, A. Sereika, J. Yang, and M. Asif Khan, *Appl. Phys. Lett.* **80**, 2020 (2002).

⁸P. Sharma and K. Sreenivas, *Appl. Phys. Lett.* **83**, 3617 (2003).

⁹V. Chivukula, D. Ciplys, A. Sereika, M. Shur, J. Yang, and R. Gaska, *Appl. Phys. Lett.* **96**, 163504 (2010).

¹⁰D. Dasgupta and K. Sreenivas, *J. Appl. Phys.* **110**, 044502 (2011).

¹¹Y. Taniyasu, M. Kasu, and T. Makimoto, *Nature* **441**, 325 (2006).

¹²B. Liu, Y. Bando, A. Wu, X. Jiang, B. Dierre, T. Sekiguchi, C. Tang, M. Mitome, and D. Golberg, *Nanotechnology* **21**, 075708 (2010).

¹³L. Shen, N. Wang, and X. Xiao, *Mater. Lett.* **94**, 150 (2013).

¹⁴J. G. Gualtieri, J. A. Kosinski, and A. Ballato, *IEEE Trans. Ultrason. Ferroelectr. Freq. Control* **41**, 53 (1994).